DEVS Simulation of Marginally Stable Systems

Ernesto Kofman and Bernard Zeigler

Abstract

In this paper we study the simulation of marginally stable systems using the methods of Quantized State Systems of first order (QSS) and second order (QSS2). We show that the simulation global error can be bounded by a magnitude which grows linearly with the time. Consequently, the direct use of QSS and QSS2 in these systems yields unstable simulation results. Therefore, we propose a modification to the methods which attempts to eliminate the mean value of the perturbations introduced by the quantization in order to avoid the unstability. All this results are illustrated with the simulation of two examples.

1 Introduction

Quantized integration methods map continuous systems into discrete event equivalents, particularly, expressed in the Discrete Event System Specification (DEVS) formalism [10]. The benefits of such mappings are numerous and include hierarchical and modular construction, seamless inclusion within object-oriented computational frameworks, and ease of mapping to parallel and distributed computing platforms.

Were these benefits to be obtained at the cost of decreased computational efficiency or degraded numerical solution properties, there might be questions raised about the applicability of these methods to current problems of interest in simulation of continuous systems. Fortunately, these concerns have been allayed an increasing body of studies that compare the quantized approaches to conventional numerical counterparts [4, 3, 6]. Indeed, such studies have shown that quantized methods can have better stability and error bound properties than do conventional methods.

Moreover, quantized integrator networks exploit the inherent efficiency of discrete event techniques that have been shown to apply in other physical abstraction such as queuing models and cellular automata. For example, speed increases of more than an order of magnitude have been demonstrated when compared to the best available numerical packages [8, 9] (perhaps leading one major developer to seek integration of discrete event methods into their offering).

Furthermore, a theory characterizing the computational demands of quantized DEVS solution in relation to conventional discrete time solutions has been developed. The theory allows prediction of the speed advantage based on a measure called "activity" which is shown to be an inherent property of a differential equation model, whether ordinary or partial [2, 1].

One issue not well addressed in the literature on numerical solutions of differential equations is that of solution of marginally stable systems. Fortunately, these 100 % energy conserving systems represent ideal forms that are not found in reality due to the second law of thermodynamics. Indeed, normally, natural systems are dissipative and marginal stability does not enter into the consideration of numerical solutions. However, there are several reasons for considering marginal stability: a) dissipation or damping might be very small compared to the oscillatory dynamics, b) marginally stable systems can be the result of applying the method of lines to hyperbolic partial differential equations, and c) mathematically, the ideal case should be addressed for completeness sake as well as for any insight it provides.

In this paper we study the simulation of marginally stable systems using the methods of Quantized State Systems [4]. We obtain an upper bound on the simulation global error for such systems that grows linearly with the time. We employ direct quantized simulation of some examples systems, using methods QSS and QSS2

[4, 3, 6], to show that such growth can occur and that it is bounded linearly in time. Consequently, the direct use of the methods in these systems yields unstable simulation results. We analyze the reason for instability and show that growth is a result of a non-zero net accumulation of the perturbations introduced by the quantization over a cycle. We conjecture that growth can be eliminated if this accumulation can be monitored and forced towards a mean of zero. This conjecture is mathematically corroborated and it is verified through a modification of the quantized integrator in which such a control feedback loop is added.

The resulting design is applied to a LC circuit and to a loss-less transmission line and shown to provide highly stable simulation with an order of magnitude speed improvement over the best equivalent Matlab/Simulink method.

2 Quantization–Based Methods

2.1 QSS–Method

Consider a time invariant ODE in its State Equation System (SES) representation:

$$\dot{x}(t) = f(x(t), u(t)) \tag{1}$$

where $x(t) \in \mathbb{R}^n$ is the state vector and $u(t) \in \mathbb{R}^m$ is an input vector, which is a known piecewise constant function.

The QSS–method [4] simulates an approximate system, which is called Quantized State System:

$$\dot{x}(t) = f(q(t), u(t)) \tag{2}$$

where $q(t)$ is a vector of *quantized variables* which are quantized versions of the state variables $x(t)$. Each component of $q(t)$ is related with the corresponding component of $x(t)$ by a hysteretic quantization function, which is defined as follows:

Definition 1. *Let $Q = \{Q_0, Q_1, ..., Q_r\}$ be a set of real numbers where $Q_{k-1} < Q_k$ with $1 \leq k \leq r$. Let Ω be the set of piecewise continuous real valued trajectories and let $x_i \in \Omega$ be a continuous trajectory. Let $b : \Omega \to \Omega$ be a mapping and let $q_i = b(x_i)$ where the trajectory q_i satisfies:*

$$q_i(t) = \begin{cases} Q_m & \text{if} \quad t = t_0 \\ Q_{k+1} & \text{if} \quad x_i(t) = Q_{k+1} \wedge \\ & \quad \wedge q_i(t^-) = Q_k \wedge k < r \\ Q_{k-1} & \text{if} \quad x_i(t) = Q_k - \varepsilon \wedge \\ & \quad \wedge q_i(t^-) = Q_k \wedge k > 0 \\ q_i(t^-) & \text{otherwise} \end{cases} \quad \text{and} \quad m = \begin{cases} 0 & \text{if } x_i(t_0) < Q_0 \\ r & \text{if } x_i(t_0) \geq Q_r \\ j & \text{if } Q_j \leq x(t_0) < Q_{j+1} \end{cases} \tag{3}$$

Then, the map b is a hysteretic quantization function.

The discrete values Q_k are called *quantization levels* and the distance $Q_{k+1} - Q_k$ is defined as the *quantum*, which is usually constant. The width of the hysteresis window is ε and, as it was shown in [5], it is better to take it equal to the quantum.

In [4] it was proven that the quantized variable trajectories $q_i(t)$ and the state derivatives $\dot{x}_i(t)$ are piecewise constant and the state variables $x_i(t)$ are piecewise linear. As a consequence, those trajectories can be represented by sequences of events and then the QSS can be simulated by a DEVS model. There, it is also shown that the use of hysteresis in QSS is necessary to ensure those properties.

The mapping of a QSS like (2) into a DEVS model can be done in several ways and one of the easiest is based on coupling principles. A generic QSS can be represented by the block diagram of Fig.1. That block diagram is composed by static functions f_i, integrators and quantizers.

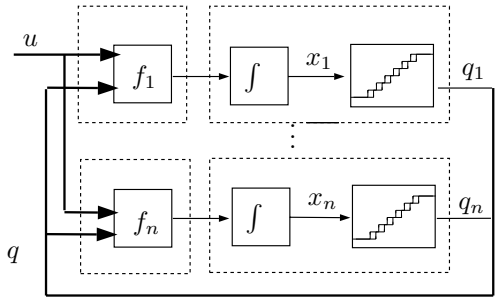

Figure 1: Block Diagram Representation of a QSS

Each pair formed by an integrator and a quantizer is called *quantized integrator* and it is equivalent to a simple DEVS model. Similarly, the static functions have DEVS equivalents and consequently, the entire block diagram has an equivalent coupled DEVS which represents it. The mentioned DEVS models can be found in [4].

Some simulation programs –PowerDEVS [7] for instance– have libraries with DEVS models representing quantized integrators and static functions. Thus, the implementation of the QSS–method consists in building the block diagram in the same way that it could be done in Simulink.

2.2 QSS2–Method

QSS only performs a first order approximation. Due to accuracy reasons, a second order method was proposed in [3] which also shares the main properties and advantages of QSS.

The basic idea of the new method, (called QSS2) is the use of first–order quantization functions instead of the quantization function given by (3). Then, the simulation model can be still represented by (2) but now $q(t)$ and $x(t)$ have a different relationship. This new system is called Second Order Quantized State System or QSS2 for short.

A first–order quantization function can be seen as a function which gives a piecewise linear output trajectory, whose value and slope change when the difference between this output and the input becomes bigger than certain threshold (Fig. 2)

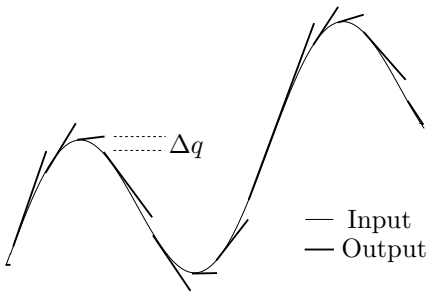

Figure 2: I/O trajectories in a *First Order* quantizer

In that way, the quantized variable trajectories are piecewise linear and the state trajectories are piecewise parabolic[1].

As before, the system can be divided into quantized integrators and static functions like in Fig.1. However, the DEVS models of the QSS2 quantized integrators are different due to the new behavior of the quantizers.

[1] In nonlinear systems this is only approximated.

Similarly, the DEVS models of the QSS2 static functions are also different since they should take into account the slopes of the piecewise linear trajectories.

The formal definition of first order quantization functions and the DEVS models associated to the QSS2 integrators and static functions can be found in [3].

Thus, the QSS2–method can be applied to ODE systems in a similar way to QSS, i.e., building a block diagram composed with the blocks representing integrators and static functions.

2.3 Properties of QSS and QSS2

There are properties –which were proven in [4] and [3]– that relates the solutions of Systems (1) and (2). These properties not only show theoretical features but also allow deriving rules for the choice of the quantization according to the desired accuracy.

The mentioned properties are stability, convergence and error bound and the corresponding proofs were built based on perturbation studies. In fact, defining $\Delta x(t) = q(t) - x(t)$, System (2) can be rewritten as

$$\dot{x}(t) = f(x(t) + \Delta x(t), u(t)) \tag{4}$$

From the definition of the hysteretic and the first order quantization functions, it can be ensured that each component of Δx is bounded by the corresponding quantum adopted. Thus, the QSS and QSS2 methods simulate an approximate system which only differs from the original SES (1) due to the presence of the bounded state perturbation $\Delta x(t)$.

The Convergence Property ensures that an arbitrarily small error can be achieved by using a sufficiently small quantization. A sufficient condition which guaranties this property is that the function f is locally Lipschitz.

The Stability Property relates the quantum adopted with the final error. An algorithm can be derived from the proof of this property which allows the choice of the quantum to be used in the different state variables.

Finally, the Error Bound is probably the most important property of quantization based methods. Given a LTI system $\dot{x}(t) = Ax(t) + Bu(t)$ where A is a Hurwitz and diagonalizable matrix, the error in the QSS or QSS2 simulation is always bounded by

$$|\tilde{\phi}(t) - \phi(t)| \leq |V||\mathbb{R}\mathrm{e}(\Lambda)^{-1}\Lambda||\mathrm{V}^{-1}|\Delta\mathrm{q} \tag{5}$$

where Λ and V are the matrices of eigenvalues and eigenvectors of A (Λ is diagonal), that is, $V^{-1}AV = \Lambda$ and Δq is the vector of quantum adopted at each component[2].

Inequality (5) holds for all t, for any input trajectory and for any initial condition.

3 QSS and Marginally Stable Systems

We analyze here the stability problems of the QSS and QSS2 methods in linear time invariant (LTI) marginally stable systems.

In the LTI case, Eq.(1) becomes,

$$\dot{x}(t) = A \cdot x(t) + B \cdot u(t) \tag{6}$$

while the QSS approximation can be written as

$$\dot{x}(t) = A \cdot q(t) + B \cdot u(t) \tag{7}$$

Defining $\Delta x(t) \triangleq q(t) - x(t)$, the last equation can be rewritten as:

$$\dot{x}(t) = A \cdot [x(t) + \Delta x(t)] + B \cdot u(t) \tag{8}$$

[2]Symbol $|\cdot|$ denotes the componentwise module of a complex matrix or vector and symbol "$\leq$" in (5) also denotes a componentwise inequality.

Let us call $\phi(t)$ to the solution of (6) starting from $x(0) = x_0$ and let $\tilde{\phi}(t)$ be a solution of (8) starting from the same initial condition

We can define the error: $\epsilon(t) \triangleq \tilde{\phi}(t) - \phi(t)$. Subtracting (6) from (8) evaluated in $\phi(t)$ and $\tilde{\phi}(t)$ respectively, it results:

$$\dot{\epsilon}(t) = A \cdot [\epsilon(t) + \Delta x(t)] \tag{9}$$

with $\epsilon(0) = 0$. Then, the error dynamics can be studied as a problem of bounded perturbations.

As in the error bound theorem [3], we shall start analyzing a the complex scalar case.

Thus, we assume that A, $\epsilon(t)$ and $\Delta x(t)$ are complex scalar numbers and we shall also consider that

$$|\Delta x(t)| \leq \Delta q \tag{10}$$

i.e. the perturbation term is bounded by a fixed bound.

When A has negative real part, Theorem 3 of [3] says that

$$\epsilon(t) \leq \frac{|A|}{|\mathbb{R}\mathrm{e(A)}|} \cdot \Delta q \tag{11}$$

Let us see what happens with the pure imaginary case. Now, Eq.(9) can be written as:

$$\dot{\epsilon}(t) = j|A| \cdot [\epsilon(t) + \Delta x(t)] \tag{12}$$

Using polar notation we define $\epsilon(t) = r(t) \cdot e^{j\theta(t)}$ and, replacing and operating we obtain

$$\dot{r}(t) + r(t) \cdot j\dot{\theta}(t) = j|A| \cdot [r(t) + \Delta x(t) \cdot e^{-j\theta(t)}] \tag{13}$$

Taking only the real part of the last equation we have:

$$\dot{r}(t) = |A| \cdot \mathbb{R}\mathrm{e}[\mathrm{j}\Delta\mathrm{x(t)} \cdot \mathrm{e}^{-\mathrm{j}\theta(\mathrm{t})}] \tag{14}$$

We can also define $\Delta x(t) \triangleq |\Delta x(t)| \cdot e^{\theta_x(t)}$ and then we get:

$$\dot{r}(t) = |A| \cdot |\Delta x(t)| \cdot \mathbb{R}\mathrm{e}[\mathrm{e}^{\mathrm{j}[\frac{\pi}{2} - \theta(\mathrm{t}) + \theta_{\mathrm{x}}(\mathrm{t})]}] \tag{15}$$

or just

$$\dot{r}(t) = |A| \cdot |\Delta x(t)| \cdot \sin[\theta(t) - \theta_x(t)] \tag{16}$$

Therefore, integrating the last equation and using the fact that $r(t) = |\epsilon|$ we arrive to:

$$|\epsilon(t)| = \int_0^t |A| \cdot |\Delta x(\tau)| \cdot \sin[\theta(\tau) - \theta_x(\tau)] d\tau \tag{17}$$

Using here (10) we arrive to:

$$|\epsilon(t)| \leq |A| \cdot \Delta q \cdot t \tag{18}$$

which bounds the error to a linear growing.

We can put (11) and (18) together in the following lemma:

Lemma 1. *Let $\epsilon(t)$ be a solution of* (9) *where A is a scalar complex with non–positive real part and $\Delta x(t)$ is bounded according to* (10)*. Then, it results that*

$$|\epsilon(t)| \leq \begin{cases} \frac{|A|}{|\mathbb{R}\mathrm{e(A)}|} \cdot \Delta q & \text{if } \mathbb{R}\mathrm{e(A)} < 0 \\ |A| \cdot \Delta q \cdot t & \text{if } \mathbb{R}\mathrm{e(A)} = 0 \end{cases} \tag{19}$$

Before jumping to the complex diagonal case, we will introduce a function which will simplify the notation. Given a $n \times n$ diagonal matrix A, we define the diagonal matrix $\beta(A,t) : \mathbb{R}^{n\times n} \times \mathbb{R} \to \mathbb{R}^{n\times n}$ so that

$$\beta_{i,i} \triangleq \begin{cases} \frac{|A_{i,i}|}{|\mathbb{R}\mathrm{e}(\mathrm{A_{i,i}})|} & \text{if } \mathbb{R}\mathrm{e}(\mathrm{A_{i,i}}) \neq 0 \\ |A_{i,i}| \cdot t & \text{if } \mathbb{R}\mathrm{e}(\mathrm{A_{i,i}}) = 0 \end{cases} \tag{20}$$

With this definition, we can rewrite Eq.(19) as

$$|\epsilon(t)| \leq \beta(A,t) \cdot \Delta q \tag{21}$$

and the following corollary becomes straightforward:

Corollary 1. *Let $\epsilon(t)$ be a solution of (9) where A is a diagonal complex matrix without eigenvalues in the right half plane and $\Delta x(t)$ is componentwise bounded according to (10). Then, the following componentwise inequality holds*

$$|\epsilon(t)| \leq \beta(A,t) \cdot \Delta q \tag{22}$$

and we are now ready to go to the general diagonalizable case:

Theorem 1. *Let $\epsilon(t)$ be a solution of (9) where A is a diagonalizable real valued matrix without eigenvalues in the right half plane and $\Delta x(t)$ is componentwise bounded according to (10). Then, the following componentwise inequality holds*

$$|\epsilon(t)| \leq |V| \cdot \beta(\Lambda,t) \cdot |V^{-1}| \cdot \Delta q \tag{23}$$

where V and Λ are a pair of eigenvectors and eigenvalues matrices of A, i.e.,

$$V^{-1} \cdot A \cdot V = \Lambda \tag{24}$$

Proof. Define $z(t)$ so that

$$\epsilon(t) = V \cdot z(t) \tag{25}$$

Then, changing coordinates in (9) we get:

$$V \cdot \dot{z}(t) = A \cdot [V \cdot z(t) + \Delta x(t)] \tag{26}$$

and then

$$\begin{aligned} \dot{z}(t) &= V^{-1} \cdot A \cdot [V \cdot z(t) + \Delta x(t)] \\ &= \Lambda \cdot [z(t) + V^{-1} \cdot \Delta x(t)] \end{aligned} \tag{27}$$

From (10) it follows that $|V^{-1} \cdot \Delta x(t)| \leq |V^{-1}| \cdot |\Delta x(t)| \leq |V^{-1}| \cdot \Delta q$ and then the system defined by (27) verifies the hypothesis of Corollary 1 which implies that

$$|z(t)| \leq \beta(\Lambda,t) \cdot |V^{-1}| \cdot \Delta q \tag{28}$$

Finally, using (25) and the equation above we get

$$|\epsilon(t)| = |V \cdot z(t)| \leq |V| \cdot |z(t)| \leq |V| \cdot \beta(\Lambda,t) \cdot |V^{-1}| \cdot \Delta q \tag{29}$$

which completes the proof. □

Theorem 1 gives a bound for the error in the simulation of a –possibly– marginally stable system. In that case, due to the presence of imaginary eigenvalues, function β will have terms which depend linearly on t.

This fact implies that the error bound grows linearly with the simulation time. It does not necessarily implies that the error will grow, but we cannot ensure that it will not.

Unfortunately, as we shall see in the examples, the error does grow in most cases.

3.1 A deeper analysis

The origin of linearly growing term can be found in the step we gave from Eq.(17) to Eq.(18).

In that step we just bounded the value of $\sin[\theta(t) - \theta_x(t)]$ to be less or equal than 1 and then we continued our analysis.

However, a more careful analysis of (17) might result in a less pessimistic conclusion.

Let us rewrite that equation as follows:

$$\begin{aligned} |\epsilon(t)| &= \int_0^t [|A| \cdot |\Delta x(\tau)| \cdot \sin(\theta)\cos(\theta_x) - \sin(\theta_x)\cos(\theta)]d\tau \\ &= \int_0^t |A| \cdot |\Delta x(\tau)| \cdot \cos(\theta_x)\sin(\theta)d\tau - \int_0^t |A| \cdot |\Delta x(\tau)| \sin(\theta_x)\cos(\theta)d\tau \end{aligned} \tag{30}$$

To see the way in which $\theta(t)$ evolves we shall come back to the imaginary part of Eq.(13), which can be written as:

$$r(t) \cdot \dot{\theta}(t) = |A|[r(t) + |\Delta x(t)| \cdot cos(\theta - \theta_x)] \tag{31}$$

and provided that $r(t) \neq 0$ we have:

$$\dot{\theta}(t) = |A|[1 + \frac{|\Delta x(t)|}{r(t)} cos(\theta - \theta_x)] \tag{32}$$

When the error is big compared with the quantum, we can see that $\theta(t) \approx |A| \cdot t + c$ where c is some constant.

In that way, $\sin(\theta)$ and $\cos(\theta)$ follow trajectories with a mean value around 0 and we might expect that the whole terms inside the integrals of (30) oscillate around 0 ... provided that there is no correlation between θ and Δx.

However –as we shall see in the examples– that correlation exists and it is strong indeed. It has to be with the fact that the sign of the perturbation introduced by the quantization is equal to the sign of the corresponding state variable derivative.

Thus, if that correlation could be eliminated in some way, we would obtain a method where the error would not grow with the time.

4 Perturbation Control

We can rewrite the first term at right hand of Eq.(30) as:

$$\int_0^t |A| \cdot |\Delta x(\tau)| \cdot \cos(\theta_x)\sin(\theta)d\tau = \int_0^t |A| \cdot \mathbb{R}\mathrm{e}(\Delta \mathrm{x}(\tau)) \cdot \sin(\theta)\mathrm{d}\tau \tag{33}$$

which can be split into small subintervals and approximated as:

$$\int_0^t |A| \cdot \mathbb{R}\mathrm{e}(\Delta \mathrm{x}(\tau)) \cdot \sin(\theta)\mathrm{d}\tau \approx |\mathrm{A}| \cdot \sum_{\mathrm{k}=1}^{\mathrm{m}} \int_{\mathrm{t_{k-1}}}^{\mathrm{t_k}} \mathbb{R}\mathrm{e}(\Delta \mathrm{x}(\tau)) \cdot \sin(\theta(\mathrm{t_k}))\mathrm{d}\tau \tag{34}$$

where $t_0 \triangleq 0$ and $t_m \triangleq t$.

Then, it results that

$$\int_0^t |A| \cdot \mathbb{R}\mathrm{e}(\Delta \mathrm{x}(\tau)) \cdot \sin(\theta)\mathrm{d}\tau \approx |\mathrm{A}| \cdot \sum_{\mathrm{k}=1}^{\mathrm{m}} \sin(\theta(\mathrm{t_k})) \cdot \int_{\mathrm{t_{k-1}}}^{\mathrm{t_k}} \mathbb{R}\mathrm{e}(\Delta \mathrm{x}(\tau))\mathrm{d}\tau \tag{35}$$

The same procedure with the second term of (30) yields:

$$\int_0^t |A| \cdot |\Delta x(\tau)| \sin(\theta_x)\cos(\theta) d\tau \approx |A| \cdot \sum_{k=1}^{m} \cos(\theta(t_k)) \cdot \int_{t_{k-1}}^{t_k} \mathbb{I}\mathrm{m}(\Delta \mathrm{x}(\tau))\mathrm{d}\tau \tag{36}$$

Thus, using (35) and (36) in (30) we have

$$|\epsilon(t)| \approx |A| \cdot \sum_{k=1}^{m} \sin(\theta(t_k)) \cdot \int_{t_{k-1}}^{t_k} \mathbb{R}\mathrm{e}(\Delta \mathrm{x}(\tau))\mathrm{d}\tau + |\mathrm{A}| \cdot \sum_{\mathrm{k}=1}^{\mathrm{m}} \cos(\theta(\mathrm{t_k})) \cdot \int_{\mathrm{t_{k-1}}}^{\mathrm{t_k}} \mathbb{I}\mathrm{m}(\Delta \mathrm{x}(\tau))\mathrm{d}\tau \tag{37}$$

Thus, if we can find a partition of the interval $[0, t]$ with points $t_0, t_1, \cdots, t_m$ where

$$\int_{t_{k-1}}^{t_k} \Delta x(\tau) d\tau = 0 \tag{38}$$

we can ensure that the error will be close to 0.

This is equivalent to say that we need $\int \Delta x$ to change its sign as fast as possible. Thus, we need to control in some way the integral of the perturbation so that it remains around zero.

We will try to achieve this by adding an extra perturbation term controlled according to the integral of the total perturbation.

The main idea is then to modify Eq.(2) adding a new perturbation term $\Delta w(t)$ so that we get:

$$\dot{x}(t) = f[q(t) + \Delta w(t), u(t)] \tag{39}$$

and then to keep the total perturbation integral around zero.

This new approximation will be called *Centered Quantized State Systems* (CQSS).

In order not to modify the essence if the QSS method we shall use a piecewise constant control $w(t)$ whose components will change simultaneously with the corresponding components of $q(t)$. We shall also restrict the value of $w_i(t)$ to be $\pm\Delta q_i$.

The control law for each component $w_i(t)$ will be, at the event times, the following one:

$$w_i(t^+) = -\Delta q_i \cdot \mathrm{sign}\left(\int_0^{\mathrm{t}} [\mathrm{q_i}(\tau) - \mathrm{x_i}(\tau) + \mathrm{w_i}(\tau)]\mathrm{d}\tau\right) \tag{40}$$

The integral can be easily calculated thanks to the particular form of the trajectory (which are piecewise constant and linear).

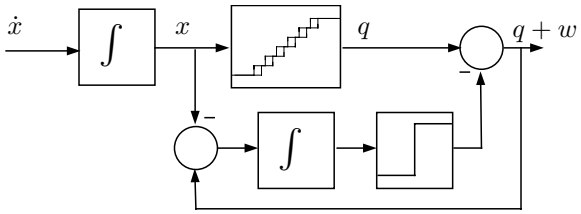

Figure 3: Centered quantized integrator

The new perturbation term $w(t)$ is bounded to Δq and then the total perturbation is bounded to $2 \cdot \Delta q$. This fact implies that the main properties of QSS are still satisfied in CQSS but now the global error bound is twice the previous one.

From the practical point of view, the only modification in the method is a change in the DEVS model of the quantized integrator. Now, we should use an extra state variable which tracks the integral of the perturbation at each transition (internal and external). The other change is in the output function, where we have to add or subtract Δq according to the sign of the mentioned integral.

5 Simulation Results

5.1 A second order system

The system

$$\begin{aligned} \dot{x}_1 &= x_2 \\ \dot{x}_2 &= -x_1 \end{aligned} \tag{41}$$

has imaginary eigenvalues $\lambda_{1,2} = \pm j$. The simulation with quanta $\Delta q_1 = \Delta q_2 = 0.1$ and initial conditions $x_1(0) = 0$, $x_2(0) = 5$ gives the results shown in Fig.4

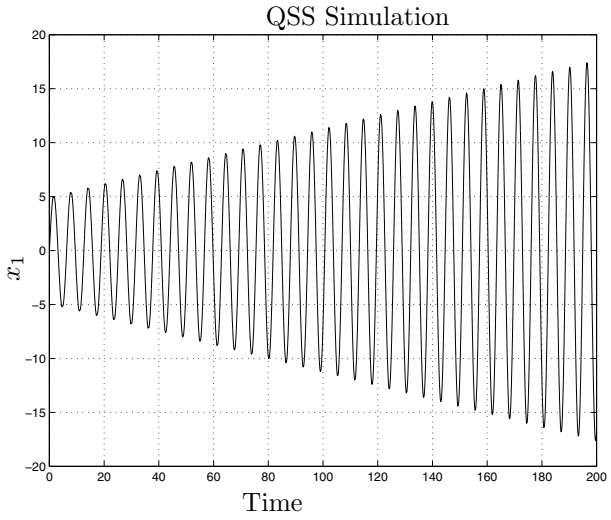

Figure 4: QSS simulation of a marginally stable system.

Theorem 1 predicts that the error is bounded by $0.2 \cdot t$ in each state variable. Figure 4 corroborates this bound (in fact the error is less than $0.07 \cdot t$).

In order to illustrate the improvement achieved by the CQSS method, we repeated the simulation of system (41) using the same paramenters than in QSS.

The results are shown in Fig.5, which are noticeably better than what was obtained with the QSS method (Fig.4).

5.2 Lossless transmission line

We shall consider now a case which unifies the main advantages of quantization based integration methods: sparsity exploitation [3] and discontinuity handling [6]. The circuit shown in Figure 6 represents a lumped model of a lossless transmission line.

The system can be described by

$$\dot{x}(t) = A \cdot x(t) + B \cdot u(t) \tag{42}$$

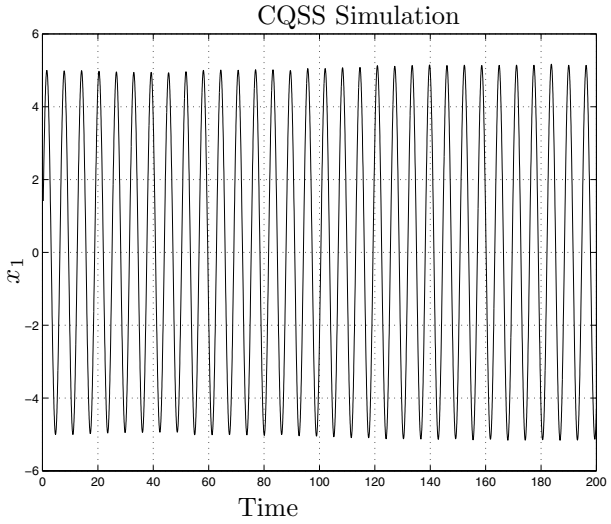

Figure 5: CQSS simulation of a marginally stable system.

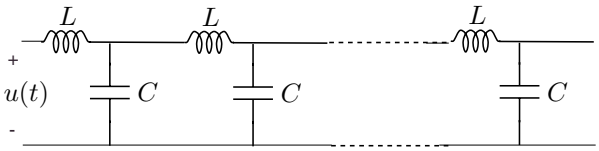

Figure 6: Lossless transmission line.

where

$$A = \begin{bmatrix} 0 & -1/L & 0 & 0 & \dots & 0 & 0 & 0 \\ 1/C & 0 & -1/C & 0 & \dots & 0 & 0 & 0 \\ 0 & 1/L & 0 & -1/L & \dots & 0 & 0 & 0 \\ 0 & 0 & 1/C & 0 & \dots & 0 & 0 & 0 \\ & & & & \vdots & & & \\ 0 & 0 & 0 & 0 & \dots & 1/L & 0 & -1/L \\ 0 & 0 & 0 & 0 & \dots & 0 & 1/C & 0 \end{bmatrix}; \quad B = \begin{bmatrix} 1/L \\ 0 \\ 0 \\ 0 \\ \vdots \\ 0 \\ 0 \end{bmatrix} \tag{43}$$

All the eigenvalues of the band structured evolution matrix A are purely imaginary. We considered 5 LC sections and we used parameters $L = C = 1$. The order of the system is then equal to 10.

The use of the same quantum Δq in all the state variables yields an error bound according to (22)

$$|\epsilon(t)| \leq [8.7953\ 11.564\ 10.918\ 11.033\ 10.696\ 10.696\ 11.033\ 10.918\ 11.564\ 8.7953]^T \Delta q \cdot t \tag{44}$$

This bound holds for any piecewise constant input trajectory $u(t)$. For the simulation, we used a pulse width modulation signal which alternates between 10 and -10, trying to produce a sinusoidal signal of 1Hz with 64 commutations by cycle.

We simulated the system using the QSS2 method with quanta $\Delta q = 0.0001$. Figure 7 shows the first 100 seconds of the evolution of $x_{10}(t)$ (the voltage in the last capacitor). According to the theoretical bound, the error is less than 0.08795 at $t = 100$.

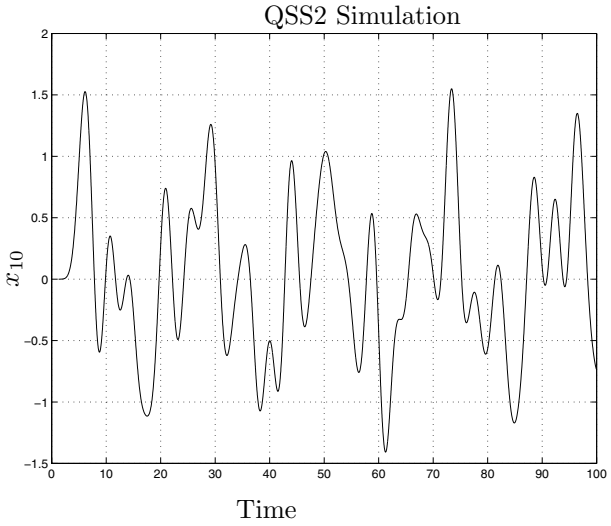

Figure 7: QSS2 simulation of a lossless transmission line.

We repeated the simulation with a quanta 10 times bigger so that the error bound at $t = 100$ is 0.8795. However, the difference with the previous simulation was always less than 0.04312 (Fig.8). That difference is in fact similar to the maximum error in the simulation.

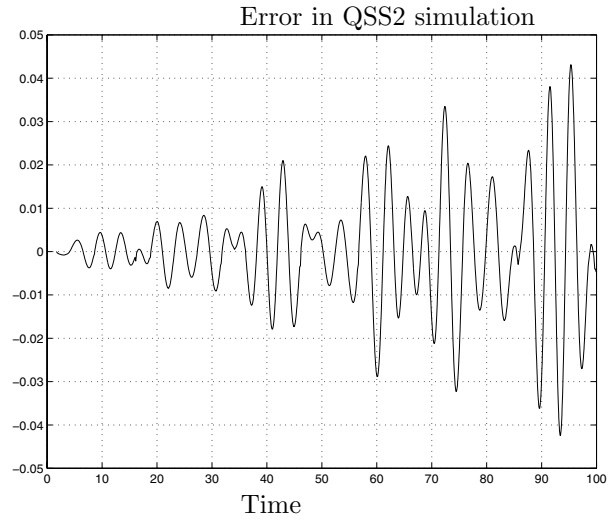

Figure 8: Error in QSS2 simulation of a lossless transmission line.

The total number of steps in the simulation with $\Delta q = 0.001$ until $t = 1000$ was 257127 (between 15000 and 61000 steps at each integrator). The input also performed 64000 commutations in that period. As the steps are local to the integrators, each step only involves calculations which affect 3 state variables. Consequently, the simulation takes about 5.3 seconds[3].

The same simulation on Matlab/Simulink using ode23s method enforcing calculations at the event times needs 329240 steps (with calculations on all the state variables), which takes about 72 seconds[4].

[3]The simulation was done with PowerDEVS [7] on a 450MHz computer.

[4]The only Matlab/Simulink algorithm which gave an acceptable result was ode23s.

In this case, the DEVS simulation was more than 13 times faster than the best result which can be obtained with Simulink.

6 Discussion and Conclusions

We have demonstrated that the reason for instability in quantized integration of marginally stable systems appears to be the result of a non-zero net accumulation of the perturbations introduced by the quantization over a cycle. Error growth can be eliminated by monitoring the net accumulation of such perturbations and forcing it toward zero with negative feedback at the event times. The resulting design appears not to significantly reduce the efficiency of the uncontrolled integrator since the time taken for achieving the same accuracy as the best equivalent Matlab/Simulink method is still significantly smaller.

There are several open questions that should be addressed in future research. Although stability properties of conventional methods in marginally stable systems has been already studied, global error bounds should be characterized in a manner similar to that done here for quantized methods. We believe that such an analysis will reveal that the same secular growth in error will be found. Finally, further analysis should be done on integration methods with error controlling feedback, to mathematical establish their desirable stability and efficiency properties in a general way.

References

[1] S. Akerar. Analysis and Visualization of Time-varying data using the concept of 'Activity Modeling'. Master's thesis, Electrical and Computer Engineering Dept, Univerisity of Arizona.

[2] Rajanikanth Jammalamadaka. Activity Characterization of Spatial Models: Application to Discrete Event Solution of Partial Differential Equations. Master's thesis, Electrical and Computer Engineering Dept, Univerisity of Arizona, 2003.

[3] E. Kofman. A Second Order Approximation for DEVS Simulation of Continuous Systems. *Simulation*, 78(2):76–89, 2002.

[4] E. Kofman and S. Junco. Quantized State Systems. A DEVS Approach for Continuous System Simulation. *Transactions of SCS*, 18(3):123–132, 2001.

[5] E. Kofman, J.S. Lee, and B. Zeigler. DEVS Representation of Differential Equation Systems. Review of Recent Advances. In *Proceedings of ESS'01*, pages 591–595, 2001.

[6] Ernesto Kofman. Discrete Event Simulation of Hybrid Systems. *SIAM Journal on Scientific Computing*, 25(5):1771–1797, 2004.

[7] Ernesto Kofman, Marcelo Lapadula, and Esteban Pagliero. PowerDEVS:A DEVS Based Environment for Hybrid System Modeling and Simulation. Technical Report LSD0306, LSD, UNR, 2003. Submitted to Simulation. Available at www.fceia.unr.edu.ar/∼kofman.

[8] J. Nutaro. *Parallel Discrete Event Simulation with Application to Continuous Systems.* PhD thesis, Electrical and Computer Engineering Dept, Univerisity of Arizona, Arizona, 2003.

[9] J. Nutaro, B.P. Zeigler, R. Jammalamadaka, and S. Akerkar. Discrete Event Solution of Gas Dynamics within the DEVS Framework: Exploiting Spatiotemporal Heterogeneity. In *Proceedings of 2003 International Conference on Computational Science*, Melbourne, Australia, 2003.

[10] B. Zeigler, T.G. Kim, and H. Praehofer. *Theory of Modeling and Simulation. Second edition.* Academic Press, New York, 2000.